CHARACTERIZATION OF SECONDARY PRODUCTS IN ARSENOPYRITE-BEARING MINE WASTES: INFLUENCE OF CEMENTATION ON ARSENIC ATTENUATION

Murciego A.[a], Álvarez-Ayuso E.[b,*], Aldana-Martínez S.C.[a], Sanz-Arranz A.[c], Medina-García J.[c], Rull-Pérez F.[c] and Villar-Alonso P.[d]

[a] Department of Geology. Salamanca University. Plza. de los Caídos s/n, 37008 Salamanca (Spain).

[b] Department of Environmental Geochemistry. IRNASA (CSIC). C/ Cordel de Merinas 40-52, 37008 Salamanca (Spain).

[c] Unidad Asociada UVa-CSIC-Centro de Astrobiología. C/ Francisco Valles 8, Boecillo (Spain).

[d] Saloro SLU. Avda. Italia 8, 37006 Salamanca (Spain).

*Corresponding author. Telephone number: +34 923219606. Fax number: +34 923219609. E-mail: esther.alvarez@irnasa.csic.es

ABSTRACT

The secondary products of an arsenopyrite-bearing mine waste dump were characterized in order to ascertain their mineralogical, chemical and environmental features and to appraise their role in the abatement of As in the environment. To this purpose, representative surface samples of weathered sulfides (including cemented phases) and hardpan samples were collected and studied by X-ray powder diffraction (XRD), polarized light microscopy, electron microprobe analysis (EMPA), micro-Raman spectroscopy and digestion, extraction and leaching methods. Scorodite, amorphous ferric arsenates (AFA), elemental sulfur, hydronium jarosite, goethite, hematite and hydrous ferric oxides were the secondary products identified in the mine wastes. The hardpan was mainly constituted by gangue minerals, including sulfides (arsenopyrite and pyrite/marcasite) with different weathering degrees, cemented by cracked yellow phases corresponding to AFA with Fe/As molar ratios of 1.14-1.85 and elemental sulfur. These cracked compounds were also the binding agent in the other cemented phases. Hydronium jarosite and Fe (oxyhydr)oxides were enriched in As, showing values of 0.19-3.98 and 0.81-7.49 wt.% As_2O_5, respectively. The As leachability and lability from hardpan and cemented phases were not decreased as compared to those from the other weathered phases not showing cementation in the mine waste dump.

Keywords: Mine wastes, arsenopyrite, secondary products, hardpan, arsenic mobility.

1. INTRODUCTION

Diverse secondary products (mostly sulfates, hydroxysulfates, (oxyhydr)oxides, arsenates and carbonates as well as some silicates and native elements) can be generated from the oxidation

of sulfidic mine wastes depending on the mine waste composition and alteration conditions. Besides, these can occur as discrete phases, coatings and cements or aggregates within the wastes, occasionally giving rise to cemented layers so-called hardpans [1].

The establishment of hardpans usually requires the succession of several events; these are the dissolution of primary minerals, the displacement of dissolved constituents, the precipitation of secondary minerals/phases (currently in the boundary region of oxidized and reduced zones) and the drying and subsequent cementation of this accumulation layer [1-3]. The precipitation and accumulation of secondary products can also happen in the oxidized zone where dissolved constituents interact with carbonates [3]. Thus, hardpans are typical of sulfide- or carbonate-rich mine wastes with miscellaneous distribution of grain sizes [2,4,5]. Mine wastes where hardpans have been developed contain frequently pyrrhotite ($Fe_{(1-x)}S$), in accordance with the high reactivity of this sulfide [2,6,7]. At times carbonates or other neutralizing materials are artificially incorporated at or just below the surface of mine wastes to induce the formation of hardpans [1,8,9]. Both natural and artificial cemented layers are known to limit pore water infiltration, to restrict oxygen diffusion and to retain toxic elements by precipitation and adsorption processes [1,3,10-12]. However, hardpans cannot be regarded as a definitive or unalterable sink for toxic elements since these could be remobilized under environmental conditions which provoke their desorption or the dissolution of precipitated minerals [13].

Different cementing agents have been identified in hardpans of sulfide mine-wastes. Those reported more frequently include Fe (oxyhydr)oxides [2,10,14,15], jarosite ($KFe_3(SO_4)_2(OH)_6$) and Fe (oxyhydr)oxides [2,10,16], gypsum ($CaSO_4 \cdot 2H_2O$) and jarosite [4,10,11], and gypsum, jarosite, and Fe (oxyhydr)oxides [4,6]. In some instances the occurrence of ferrous sulfates such as melanterite ($FeSO_4 \cdot 7H_2O$) and rozenite ($FeSO_4 \cdot 4H_2O$) has been also detected, mainly as pore-filling materials [6,13]. The presence in hardpan cements of As-minerals/phases such as scorodite ($FeAsO_4 \cdot 2H_2O$), amorphous ferric arsenates (AFA) and amorphous ferric sulfoarsenates [3,17], as either binding or pore-filling materials, is also less frequent, and related to the substantial occurrence of arsenopyrite (FeAsS) in mine wastes.

Many researches have been dedicated to study the oxidation processes and weathering phases of arsenopyrite [e.g., 18-28], at either laboratory or field conditions, establishing its main dissolution pathways and conditions, and identifying its most relevant secondary As products (mostly As oxides, Fe arsenates, Fe sulfoarsenates and sulfoarsenites, Ca and Mg arsenates, and Zn, Pb and Cu arsenates). In any case, the occurrence and prevalence of secondary phases and their role in the As abatement in the surrounding environment are

greatly determined by the original mineralogy of the exploited deposit and by the local or regional climatic conditions. Thus, the study of arsenopyrite-bearing mine wastes in regions with warm semiarid or arid climates has revealed that such circumstances favor the relatively fast formation of hematite (α-Fe_2O_3) which traps tightly As, considering this immobilization very efficient even for a long-term perspective [29]. Under more extreme climatic conditions, as those typical of desert regions where high-temperature and low-water availability dominate, the oxidation of sulfides hardly occurs, being the mechanical dispersion of particles the mechanism responsible for As spreading [5]. In this regard, it has been found that the arsenopyrite oxidation takes place to a greater extent in water than in air [20,28,30]. The ready dissociation of oxygen on arsenopyrite surface, which leads to the prompt oxidation of Fe and As sites, has been proposed as the oxidation mechanism of arsenopyrite in presence of water [28]. Furthermore, its concurrency is regarded as crucial to such an extent that the inhibition of arsenopyrite oxidation is hypothesized when humidity is removed [28]. By contrast, under temperate climates arsenopyrite undergoes significant weathering when exposed to atmospheric conditions. The mobility of released As is controlled by the precipitation and dissolution of different secondary phases, with their geochemical dynamics being governed by seasonal dry-wet cycles and local microenvironments [25,31-34]. Of secondary products, Fe arsenates are the most common in weathered arsenopyrite-bearing mine wastes, including both well-crystallized and amorphous phases [21]. Particularly, scorodite is the most frequent one, having been found in many mining areas around the world [21]. It is highly stable under acid oxidizing conditions, but dissolves incongruently from pH about 3, with the simultaneous precipitation of Fe (oxyhydr)oxides, which act as a sink for the released As [23]. Kaňkite ($Fe_3AsO_4 \cdot 3.5H_2O$), although much rarer than scorodite, has been reported coexisting with scorodite [25,35-37] or replacing it in places where moisture persists for long periods of time (months) [34]. Amorphous Fe arsenates also appear frequently associated with these two crystalline phases [25,26,38,39], but present much higher solubilities [23]. These compounds are considered metastable and a precursor of scorodite [40]. This transformation takes place quickly at pH 1 [40,41], being delayed exponentially with the rising pH [40]. In locations where Ca is available, and pH values are slightly higher, yukonite ($Ca_7Fe_{11}O_{10}(AsO_4)_9 \cdot 24.3H_2O$) and arseniosiderite ($Ca_2Fe_3O_2(AsO_4)_3 \cdot 3H_2O$) occur [39,42-44]. Particularly, arseniosiderite is stable at pH values ranging from 3.5 to 7.5 when solutions are saturated with regard to soluble Ca minerals [42], whereas yukonite is considered a nanocrystalline precursor of arseniosiderite, showing some Ca deficiency with respect to this latter [42]. These Fe-Ca arsenates are also commonly found together with pharmacosiderite ($KFe_4(OH)_4\ (AsO_4)_3 \cdot 6\text{-}7H_2O$) or minerals of the pharmacosiderite group [21,39,43,44]. Specifically, pharmacosiderite forms under moist

neutral to alkaline environments when dissolved K and Fe/As molar ratios > 1 are present [34]. Nevertheless, at higher Fe/As molar ratios (> 2) the precipitation of Fe (oxyhydr)oxides would be favored, which effectively scavenge the released As [21,34]. Like yukonite, minerals of the pharmacosiderite group are considered less stable than arseniosiderite, especially at high Ca activity values, being also transformed into it under such conditions [43,45]. Although less frequently, Fe sulfoarsenates are also found in weathered arsenopyrite-bearing mine wastes, especially when the presence of pyrite (FeS_2) is also considerable, as their formation needs acid conditions and relatively important concentrations of dissolved sulfate [34]. The main Fe sulfoarsenates reported in this kind of wastes include bukovskýite ($Fe_2(AsO_4)(SO_4)(OH)\cdot 7H_2O$) [34,38,46,47], zýkaite ($Fe_4(AsO_4)_3(SO_4)(OH)\cdot 15H_2O$) [34,36,46,48] and tooeleite ($Fe_6(AsO_3)_4(SO_4)(OH)_4\cdot 4H_2O$) [39,46], together with beudantite ($PbFe_3(AsO_4)(SO_4)(OH)_6$) [49-52] in wastes where the presence of galena (PbS) is also significant. Of them, both bukovskýite and zýkaite require persistent damp conditions to be formed [34]. These two minerals have been described as products of the bacterial oxidation process [46] as happens with tooeleite [46,53]. In this regard, microorganisms commonly present in the acid mine drainage (AMD) are known to play an active role in the oxidation of Fe- and S-minerals [20]. In particular, acidophilic Fe-oxidizing bacteria such as *Acidithiobacillus ferrooxidans* and *Leptospirillum ferrooxidans* have been reported to greatly enhance the arsenopyrite oxidation process [18,54], with such improvement being attributed to the oxidation of Fe(II) to Fe(III). In this respect, Fe(III) has been proven to oxidize arsenopyrite faster than dissolved oxygen in acidic media (at least one order of magnitude faster) [19]. Moreover, under such conditions the rate of arsenopyrite oxidation rises importantly with the growing concentration of dissolved Fe(III) [55]. In addition to this indirect mechanism, where microorganisms catalyze the arsenopyrite oxidation process through the oxidant regeneration, it has been also reported the involvement of a direct mechanism via the attachment of microorganisms to the mineral surface, which provokes corrosion pits [18,56,57]. Although *Acidithiobacillus ferrooxidans* and *Leptospirillum ferrooxidans* are typical of the AMD of temperate regions [58], and have focused a lot of attention, many other different microorganisms can be present in other regions as the dominant microbial community in the AMD is dependent on climatic conditions and physicochemical characteristics of the local microenvironments such as pH, ionic strength and temperature [58-61].

In spite of this amount of work and knowledge on arsenopyrite oxidation pathways, conditions and products, the studies of mine wastes where the weathering of arsenopyrite has led to the development of hardpans are scarce [3,17]. More research is basic in this regard to elucidate

their composition and properties and to assess their impact on the abatement of environmental dangers.

The main objectives of this work were to establish the mineralogical, chemical and environmental characteristics of the secondary products present in a former arsenopyrite-bearing mine waste dump where cemented phases/layers occurred and to evaluate their role in the attenuation of As in the environment.

2. MATERIALS AND METHODS

2.1. Study area

The former Barruecopardo mine is situated 2 km south of Barruecopardo, a village in the NW of the province of Salamanca (Spain). This mine worked the main tungsten deposit in Spain, mainly during the 1930-1960 and 1960-1982 periods, reaching its highest production between 1942 and 1945. Artisanal mining was performed in the first period of exploitation, whereas mechanized systems were employed in the second one. The deposit is constituted by NNE-SSW and subvertical quartz veins, with thickness typically between 2 and 30 cm, found in intra-granitic bands of parallel arrangement; exceptional is the thickness of the main vein, ranging from 1 to 5 m. The mineral association of quartz veins is mainly composed of scheelite ($CaWO_4$), arsenopyrite, wolframite ($(Fe,Mn)WO_4$) and pyrite/marcasite (FeS_2), with the two former being the most abundant, accompanied by feldspar, mica and apatite. Mining activities generated about several millions of tons of wastes that were accumulated in dumps around the open pits. Nowadays, remnants of the past mining activities (ancient processing plant, mine dumps, open pits, etc.) are still perceivable in the area. Hence, this area was chosen to perform the study because in this location there are arsenopyrite-rich mine wastes that have undergone more than 60 years of weathering, giving rise in some instances to hardpans derived specifically from the alteration of this mineral.

The climate in Barruecopardo is classified as Csb by the Köppen-Geiger system. This is a Mediterranean climate with dry and warm summers. Particularly, Barruecopardo has a warm temperate climate, with the winter period being much rainier than the summer period. Its annual average temperature and rainfall are 12.2 °C and 726 mm, respectively. During the year, the temperature generally varies within 1-30 °C, rarely decreasing below -4 °C or increasing above 35 °C. In the warm season (from mid-June to mid-September) the average temperature attains 20.0 °C and in the cold season (from mid-November to early March) the average temperature is 5.4 °C. November through February is the rainiest time, with a monthly

average precipitation of 92 mm, whereas the driest months are July and August, where precipitation drops to 10 mm.

Taking into account the great influence of climatic conditions on arsenopyrite weathering, the characterization of mine wastes of this location should only be extended to regions with Mediterranean climate.

2.2. Sampling

The most ancient waste dump present in the study area was considered for sampling. It was composed of host rocks and/or hydrothermal veins fragments of very different size (from mm to tens of cm), comprising mostly gangue minerals, including sulfides (arsenopyrite and pyrite/marcasite), and diverse weathering products of these latter. Also an exposed hardpan with a thickness of roughly 2 cm was present. This hardpan exhibited two zones or layers. The upper layer was about 0.5 cm thick and showed grayish colors, whereas the bottom layer was about 1.5 cm thick and showed greenish/yellowish colors. Approximately 30 samples were collected from this waste dump. These comprised surface samples with sulfides showing different weathering degrees, with some of them containing cemented phases, and hardpan samples (Fig. 1).

2.3. Mineralogical and chemical characterization of mine wastes

Mine waste samples were analyzed by X-ray diffraction (XRD), polarized light microscopy, electron microprobe analysis (EMPA) and micro-Raman spectroscopy to establish their mineralogical and chemical characterization.

The analyses by XRD were carried out on unoriented powder samples employing the monochromated Cu Kα radiation (40 kV and 30 mA) on a D8 Advance Bruker diffractometer, and performing scans over a range of 2-3° to 65-70° 2θ with a 2θ step size and a counting time per step of 0.04° and 1 s, respectively. The analyses by polarized light microscopy were performed on polished thin sections of samples using a Nikon Eclipse E400 POL optical microscope functioning in reflection and transmission modes. Spot chemical analyses and electron backscatter images were obtained by EMPA. To this end carbon-coated polished thin sections of samples were analyzed in wavelength-dispersive mode by means of a JEOL Superprobe JXA-8900M electron probe micro-analyzer working at a beam current of 50 nA and an accelerating voltage of 20 kV, and using a spot size of 1-5 µm and peak and background counting times of 10 s and 5 s, respectively. The analyzed elements were: Al, Si, Fe, P, As, S, K, Na and Mn. The analyses by micro-Raman spectroscopy were performed on polished thin sections of samples using a KOSI Holospec f/1.8i spectrometer equipped with a Nikon Eclipse E600 microscope, a laser REO LSRP-3501 He-Ne (632.8 nm) operating at 1 mW as excitation

source and an Andor DV420A OE CCD camera as detector. The laser beam was focused on samples by x100 objective lens. The overall spectra resolution was 5 cm^{-1}.

2.4. Environmental characterization of mine wastes

The following parameters were determined to establish the environmental characterization of mine wastes: pH, total As content, leachable As content, labile As content and toxicity. Different groups of samples were subjected to this characterization. These comprised samples containing pyrite/marcasite and their weathering products, samples containing arsenopyrite and its weathering products, cemented phases, hardpan, upper zone of hardpan and bottom zone of hardpan. In addition, an experimental design was established to determine the influence of pH on As leachability from the different groups of mine wastes considered in this study.

The pH of mine wastes was measured potentiometrically in triplicate on ground samples (< 0.250 mm) using the water-saturated paste procedure. The total As content of mine waste samples was determined in triplicate by acid digestion of ground samples (< 0.100 mm) with aqua regia in a Milestone Ethos Plus microwave oven operating at 190 °C for 15 min. After digestion, As was analyzed in the resulting extracts by inductively coupled plasma-atomic emission spectrometry (ICP-AES) by means of a Varian 720-ES spectrometer. Standard reference materials (SRM 2709a and SRM 2711a) were employed to assess the accuracy of the determination method; recoveries within the range 90-110 % were obtained. The leachable As content of mine waste samples was determined pursuing the European leaching test EN-12457-4 [62]. Thus, crushed samples (< 10 mm) underwent in triplicate a shaking stage of 24 h with deionized water employing a liquid:solid ratio of 10 L kg^{-1} in a rotary shaker functioning at 10 rpm. After the sedimentation of suspensions, 0.45 µm membrane filters were employed to filtrate supernatants. The obtained leaching extracts were analyzed for As by ICP-AES. The labile (soluble + non-specifically adsorbed) As content of mine waste samples was appraised following the method of Wenzel et al. [63]. Accordingly, crushed samples were subjected in triplicate to a shaking stage of 4 h with 0.05 M $(NH_4)_2SO_4$ employing a liquid:solid ratio of 25 L kg^{-1} in a rotary shaker. After sedimentation and filtration, the obtained extracts were analyzed for As by ICP-AES. Toxicity of mine wastes was established according to the TCLP (Toxicity Characteristic Leaching Procedure) test method. Thus, crushed waste samples (< 9.5 mm) underwent in triplicate an agitation period of 18 h with buffered acetic acid (pH 4.93 ± 0.05) in a vertical rotary shaker (30 rpm), using a liquid:solid ratio of 20 L kg^{-1}. After sedimentation and filtration, the obtained extracts were analyzed for As by ICP-AES. The influence of pH on As leachability from the different groups of mine wastes was studied at five pH levels (1, 2, 4, 6

and 8). For this purpose, crushed samples were subjected in triplicate to shaking periods of 18 h with aqueous buffered solutions at the indicated pH values in a rotary shaker, employing a liquid:solid ratio of 20 L kg^{-1}. After sedimentation and filtration, the obtained leachates were analyzed for As by ICP-AES.

3. RESULTS AND DISCUSSION

3.1. Mineralogical and chemical characterization of mine wastes

The XRD analyses (Fig. 2) revealed that the main mineral phases occurring in mine wastes were arsenopyrite, pyrite, marcasite, quartz, muscovite and albite, as gangue minerals, scheelite and wolframite, as ore minerals, and scorodite, hydronium jarosite ($(H_3O)Fe_3(SO_4)_2(OH)_6$), goethite (α-FeO(OH)), hematite and elemental sulfur, as secondary minerals. In the samples of hardpan and cemented phases mainly gangue minerals were identified, whereas only scorodite and/or elemental sulfur were detected as secondary minerals.

Polarized light microscopy analyses in transmitted and reflected light and electron backscatter images (Figs. 3 and 4) allowed to identify arsenopyrite, pyrite and marcasite as the sulfide minerals present in mine wastes, with the former being the prevailing sulfide and the most weathered of them. These minerals were present as unweathered euhedral crystals, in relicts showing corroded borders and as entirely weathered crystals that preserved their original shape. The observed secondary products were scorodite, goethite, hematite, jarosite-group minerals, yellowish phases (in transmitted light) of cracked appearance, and cracked phases of intense red color (in transmitted light). Scorodite exhibited mainly a microcrystalline texture. The yellowish phases appeared in concentric bands showing mud-cracks. Both occurred on arsenopyrite crystal borders and along arsenopyrite cracks. The yellowish phases also appeared on grains of sulfides and silicate minerals, cementing them. Goethite, hematite and cracked red phases pseudomorphically substituted for pyrite/marcasite, being frequent the presence of relicts of these sulfides in all of them. The minerals of the jarosite group occurred on crystal borders and along fissures of pyrite/marcasite. The minerals detected in the hardpan layer were arsenopyrite (partially or completely altered), pyrite/marcasite and grains of quartz, muscovite and feldspar. All of them were bound by a yellowish phase of cracked texture. This phase was also identified as the binding material in cemented phases. The observations in transmitted light with crossed polarizers revealed that this phase was of amorphous nature.

A total of 121 spot chemical analyses were done by EMPA on sulfide weathering products (Table 1). Scorodite exhibited Fe_2O_3 (average value: 35.4 wt.%) and As_2O_5 (average value: 47.6

wt.%) contents very similar to its theoretical values (34.6 wt.% and 49.8 wt.%, respectively), with only trace or undetectable amounts of the other considered elements, except for S which showed a faintly increased level (average value: 1.0 wt.% SO_3). The main major elements present in the yellow cracked phases were Fe and As. Their Fe_2O_3 (32.5-50.5 wt.%) and As_2O_5 (29.4-48.3 wt.%) contents did not exhibit a precise stoichiometry, with Fe/As molar ratios being comprised within the range 1.14-1.85. Such composition together with their amorphous character and their important degree of hydration suggests that these phases corresponded to AFA. These compounds can accommodate different elements in their composition [21]. Of the other analyzed elements, only S reached considerable values (1.4-22.1 wt.% SO_3). Therefore, these yellow cracked phases could be high-sulfur AFA known as amorphous ferric sulfoarsenates. The Fe_2O_3 (average value: 44.2 wt.%) and SO_3 (average value: 33.3 wt.%) contents in the minerals of the jarosite group resulted in Fe/S molar ratios (average value: 1.33) lower than the theoretical value (1.5), showing a deficit in Fe. Jarosites deficient in Fe, with Fe/S molar ratios significantly lower than that conforming to the ideal stoichiometry, are quite common [64]. Thus, Fe/S ratios about 1.10-1.30 have been already reported [64]. The studied jarosites were also deficient in K (average value: 0.70 wt.% K_2O) and Na (average value: 0.86 wt.% Na_2O) as compared to the ideal formulas of the typical jarosite ($KFe_3(SO_4)_2(OH)_6$) and natrojarosite ($NaFe_3(SO_4)_2(OH)_6$) (9.4 wt.% K_2O and 6.4 wt.% Na_2O, respectively). Such deficiencies in K and Na together with their important degree of hydration suggest that these mineral phases were hydronium jarosites as was revealed by XRD. On the other hand, these minerals presented an enrichment in As (average value: 0.91 wt.% As_2O_5). It is well know that jarosites are able to retain As [65,66], which can be either adsorbed on the mineral surface or incorporated into the mineral structure substituting for sulfate [66]. A high negative correlation ($|R| = 0.93$; $p < 0.001$) was found between their SO_3 and As_2O_5 contents, pointing out the important contribution of this latter mechanism. In any case, the pH range in which jarosites are stable is quite narrow (up to about pH 3) [65]. Goethite and hematite, according to their known capacity to retain As, were also enriched in this element (average values: 2.23 and 1.32 wt. % As_2O_5, respectively). Additionally, other elements showed also relatively important levels in these minerals, mainly Si (1.67 and 3.62 wt. % SiO_2, respectively) and Al (1.72 wt. % Al_2O_3 in goethite). The cracked red phases exhibited, in general, lower Fe_2O_3 contents (50.8-78.8 wt.%) than those corresponding to goethite and hematite, indicating a higher degree of hydration. Their As_2O_5 contents (3.95-7.49 wt.%) were in turn higher than those found typically for the As retention by goethite and hematite (up to about 2.5 and 1.5 wt.% As_2O_5, respectively) [67-69], pointing out an improved As retention capacity as that

shown by amorphous or low-ordered compounds. These features suggest the occurrence of hydrous ferric oxides in such cracked red phases.

Sulfide weathering products were also analyzed by micro-Raman spectroscopy. The representative micro-Raman spectra of analyzed phases are shown in Fig. 5. The micro-Raman spectrum of the mineral identified as scorodite showed strong sharp peaks at about 180, 800 and 900 cm^{-1}, with the two latter corresponding to the typical As-O stretching vibration bands of this mineral [66]. Also other minor bands at 250, 290, 335, 380, 422 and 450 cm^{-1} were observed in agreement with other scorodite spectra reported previously [37,70]. The yellow cracked phases exhibited a micro-Raman spectrum with most bands appearing below 500 cm^{-1}, i.e. at 151, 185, 217, 245, 438 and 471 cm^{-1}. These bands are typical of the S-S vibration of elemental sulfur [71]. Additionally, a broad band within the typical frequency region of arsenate (700-950 cm^{-1}) [71] was also observed. These data are consistent with the occurrence of mixtures of elemental sulfur and AFA rather than with the occurrence of amorphous ferric sulfoarsenates. The minerals of the jarosite group showed spectral bands at 222, 304, 349, 420, 450, 568, 621, 1008, 1100 and 1157 cm^{-1}. These bands agreed well with those reported for hydronium jarosite [72]. Additionally, a band at about 820 cm^{-1} was also present. This was in the region where the bands of As-O stretching modes appear [73], being in accordance with the presence of retained As. The micro-Raman analyses performed on Fe (oxyhydr)oxides revealed that these phases are mainly constituted by goethite. Thus, Raman peaks characteristic of goethite [74,75] appeared at 244, 300, 389, 480, 552 and 688 cm^{-1}, with that at 389 cm^{-1} being the strongest. In addition, a broad peak at about 840 cm^{-1} was also present. This band is consistent with the occurrence of adsorbed arsenate [76,77]. The analyses on Fe (oxyhydr)oxides also revealed the presence of hematite, showing its characteristic Raman peaks [74] at 225, 245, 294, 408, 495, 610 and 1318 cm^{-1}, with those at 225, 294 and 408 cm^{-1} being the most intense. Another peak at 660 cm^{-1} was also observed. This peak has been previously found and related to structural disorder [77]. No other minerals were detected by the analyses performed specifically on the cracked red phases, indicating that these phases were mainly composed of different mixtures of goethite and amorphous ferric oxides.

According to the mineralogical and chemical characterization performed on mine wastes scorodite, AFA, elemental sulfur, hydronium jarosite, amorphous/low ordered hydrous ferric oxides, goethite and hematite are the main secondary products arising from the long-term weathering of these arsenopyrite-bearing mine wastes.

Scorodite, AFA and amorphous/low ordered hydrous ferric oxides are frequently found associated in this kind of wastes after different periods of alteration (≤ 50-≥ 500 years)

occurring under acidic conditions [25,26,38,39], favored by the ongoing sulfide alteration. Of them, AFA are the first phase that precipitates from solutions with a wide range of Fe/As molar ratios (1-4) at low pH values [40]. Nevertheless, AFA are metastable and transform to scorodite from pH about 1 and to hydrous ferric oxides from pH about 2 through incongruent dissolution [40]. The transformation of AFA into scorodite is very rapid at pH about 1, but slows down exponentially with the increasing pH [40].

Although less often, elemental sulfur has also been reported as an important common secondary product resulting from the alteration of arsenopyrite-rich mine wastes [25,37,78]. In addition to the occurrence of elemental sulfur in advanced phases of arsenopyrite oxidation, elemental sulfur has also been reported in the initial steps of the weathering process [79] and described as an intermediate oxidation product [80]. In the initial phases of weathering elemental sulfur appears forming thin layers or patches on arsenopyrite [54,79,81]. When oxidation progresses it usually occurs as microscopic crystals or forming grainy aggregates that pseudomorphise arsenopyrite [25,37]. Such elemental sulfur pseudomorphs appear frequently rimmed or surrounded by other secondary phases, mostly scorodite [25,37,78], what differs from the present study in which elemental sulfur was found associated with AFA. In this case AFA was the dominant arsenopyrite weathering product and constituted the cementing material. In this regard, unlike what happens in these mine wastes, scorodite is usually the secondary As phase derived from the alteration of As-rich mine wastes constituting the binding agent in cemented masses or crusts developed in mine wastes [25,34,78,82,83]. Although much more rarely, also other secondary As phases have been identified as cementing materials, including AFA [25], kaňkite [25,34] and bukovskýite [34], with this latter appearing only in cements of the interior of dumps. As regards hardpans, the secondary As phases reported as binding agents in these cemented layers include both scorodite and AFA, with their predominance being dependent on the specific pH of the acid microenvironment [3]. In any case, these phases evolve to hydrous ferric oxides when weathering progresses and the pH of pore waters attains circumneutral values [3]. Also the presence of amorphous ferric sulfoarsenates has been reported in hardpans, but in this case as a pore filling material [17].

Jarosite group minerals are typical secondary products in sulfidic mine wastes, being also found in arsenopyrite-bearing mine wastes in which other Fe sulfides, especially pyrite, are present [38,52,84,85]. Typically, these minerals occur as over-growths on Fe sulfide minerals in the form of grains or nodules of variable size [38,84,85]. Although hydronium jarosite is not among the most common minerals of this group, its presence in acid mine wastes is not infrequent either [38,52,85,86]. Its reported As contents (0.16-0.90 wt.% As_2O_5 [52]) are similar

to that found in the studied area (average value: 0.91 wt.% As_2O_5). Such contents are also in line with those reported for the typical jarosite (0.04-3.35 wt.% As_2O_5[25,52]). Nevertheless, hydronium jarosite is much more soluble than this latter [87], and, therefore, a less efficient reservoir for As. Another hydroxysulfate found in weathered sulfidic mine wastes, quite often associated with jarosite group minerals, is schwertmannite ($Fe_8O_8(SO_4)(OH)_6$). Although the formation of schwertmannite is known to be kinetically favored from the oxidation of Fe sulfides with regard to other ferric minerals/compounds, this is a metastable phase and transform to jarosite minerals or Fe (oxyhydr)oxides, depending on the pH conditions [87-90]. Furthermore, in ferric sulfate media with As/Fe molar ratios above 0.15-0.2 the formation of AFA takes place instead of schwertmannite [91,92], due to the positioning effect of As in its the oxidized state that avoids or restricts the nucleation of schwertmannite [92]. Therefore, apart from its metastability, its absence in the studied area as well as in other oxidized mine wastes in which the occurrence of arsenopyrite was considerable is explained and expected. Conversely, the presence of Fe (oxyhydr)oxides is almost ubiquitous in sulfidic mine wastes containing arsenopyrite, with hydrous ferric oxides, goethite and hematite being the most common [29,31,38,43]. These phases scavenge As in important amounts, especially hydrous ferric oxides. Their As contents found in this study (3.95-7.49 wt.% As_2O_5) agree well with those reported previously in literature ($\leq$ 0.1-24.7 wt.% As_2O_5 [25,38,43,44]).

3.2. Environmental characterization of mine wastes

The environmental parameters determined on the different mine waste samples are shown in Table 2. All the considered samples had pH values within the range 2.6-3.4. In general, pH values below 4 indicate that materials are acid producing. The lowest pH was shown by the sample containing arsenopyrite and its weathering products, which is consistent with the occurrence of scorodite. It is well known that the minimum solubility of scorodite is close to pH 3, from which it dissolves incongruently [23].

The leachable As content of mine waste samples as determined following the European leaching test EN-12457-4 [62] reached high values, varying between 76.7 and 14.5 mg kg^{-1} according to the following sequence: arsenopyrite and its weathering products > upper zone of hardpan > hardpan > cemented phases > bottom zone of hardpan > pyrite/marcasite and their weathering products, although differences were not significant ($p > 0.05$) between most correlative samples. Except for pyrite/marcasite and their weathering products, all the other samples (arsenopyrite and its weathering products, hardpan and their different layers, and cemented phases) showed leachable As contents higher than the limit established for wastes to be accepted at landfills for hazardous wastes (25 mg kg^{-1} [93]). Therefore, a treatment to

reduce their leachable As contents down to the indicated limit would be required even for their disposal in this type of landfills. Such leachable As contents, although being high, only represented small fractions (about 0.03-0.06%) of total contents, which varied between 25.6 and 5.0%. Therefore, even if the hardpan as a whole accumulated important amounts of As (7.9%), the As leachability from it was of the same order as those from the other groups of phases, either cemented or not, that integrated the studied mine dump.

The labile As content of mine waste samples showed values comprised between 220 and 17.8 mg kg^{-1}, with the highest level corresponding to the sample containing arsenopyrite and its weathering products and the lowest to the sample containing pyrite/marcasite and their weathering products. In any case, all of the mine waste samples exhibited very risky labile As contents, even if they represented only a reduced fraction (about 0.04-0.29%) of total As. This As pool, which accounts for soluble and non-specifically adsorbed As, has been suggested as the most important in relation to environmental risks [63,94]. Again the As lability from the cemented phases and layers was not reduced with respect to those from the other groups of phases present in the studied mine dump.

According to the TCLP test, only the As concentration released from the mine waste sample composed of arsenopyrite and its weathering products (6.3 mg L^{-1}) surpassed the regulatory limit set for toxic characterization (5 mg L^{-1}), and, therefore, is characterized as toxic. The As concentration released from cemented phases and hardpan samples (4.4-2.4 mg L^{-1}), although not exceeding the established limit, attained values relatively close to the toxic characterization, whereas the sample integrated by pyrite/marcasite and their weathering products would have required to increase the discharge of As in one order of magnitude.

Generally, hardpans in mine dumps include Fe (oxyhydr)oxides in their composition, being either the main or one of the main constituents of the cementing phase [2,4,6,10,14-16]. It is well know that Fe (oxyhydr)oxides have an important capacity to adsorb different toxic trace elements, including As. The adsorption of As by them mostly takes place specifically via inner-sphere complexes [95]. Moreover, when Fe (oxyhydr)oxides are generated in situ, as happens in mine scenarios, their capacity to remove As is greatly increased, as this element can be incorporated into the Fe (oxyhydr)oxide precipitates [96,97]. The important amount of As susceptible of being retained by these phases and the main mechanisms involved in its retention, either specific adsorption or incorporation into the solid phase, explain the ability usually shown by hardpans to lessen the mobility of As. In the hardpan and cemented phases of the studied mine waste dump AFA were identified as the occurring cementing material. These compounds are metastable and greatly soluble [40]. Anyway, their stability and

solubility are dependent on their Fe/As ratio. Thus, their stability turns out to be broader and their solubility lower with the increasing Fe/As ratio [98]. Solubility differences of about 100-1000-fold have been found between precipitates with Fe/As ratios varying from 1 to ≥ 4 within a broad range of pH values [98]. The AFA occurring in the hardpan and cemented phases showed Fe/As molar ratios comprised within the range 1.14-1.85 (average value: 1.41). Such Fe/As ratios were relatively close to those of AFA having higher solubilities, what explains the levels of As solubilization showed by these cemented phases and layers. This is in line with the unsatisfactory performance exhibited by AFA for the As restraint in mine discharges [23]. In this regard, much lower solubilities have been found for scorodite (about 1-7 orders of magnitude lower), which would make the precipitation of this mineral suitable to appropriately treat mine discharges [23]. Nevertheless, the great dependence of the scorodite solubility with pH [23] would be the main constraint to the lasting effectiveness of such a treatment. Thus, the long-term As retention by hardpans whose cement composition was based on scorodite, on AFA or on mixtures of both was not expected either in other historical arsenopyrite-bearing mine tailings [3]. The progression of sulfide weathering has been found to play a decisive role in the cement formation, composition and stability as it determines the pH conditions and the availability of Fe(III) and As(V) [3]. It is known that AFA dissolve incongruently to produce ferrihydrite as the pH is raised from pH values about 2 [23,40,41]. As the Fe/As ratio of precipitates increases, the occurrence of ferrihydrite rises and that of AFA decreases, with these latter disappearing in precipitates with Fe/As ratios of 5 and greater [41]. The increase in the Fe/As ratio of precipitates enhances the As stabilization by them [41]. Therefore, the cemented phases and layers present in the studied mine dump could be expected to be dissolved when local conditions were propitious for the formation of ferrihydrite. The As released by the dissolution of AFA could be immobilized in great extent by this freshly precipitated phase, which could reach As(V)/Fe molar ratios up to about 0.7 [96].

The influence of pH on As leachability from mine wastes considered in this study is shown in Table 3. Differences in As solubilization within the same group of mine wastes were found not significant ($p > 0.05$) between pH values of 6 and 8. Nevertheless, below them the As release increased drastically from all the samples with the decreasing pH, pointing out the significant role played by pH in As leachability. For most of the sample groups the As solubilization was increased from pH 6-8 to pH 4, 2 and 1 about 2-10, 20-50 and 125-250 times, respectively. The sample composed of arsenopyrite and its weathering products showed the least pronounced rises, attaining at the indicated pH values (4, 2 and 1) As releases about 2, 5 and 15 times as much as those at pH 6-8.

Different processes can explain the increased As release from mine waste samples with the decreasing pH. At pH values < 3 the solubilization of Fe (oxyhydr)oxides can take place, releasing the As previously retained by them. Additionally, Fe(III) becomes free to act as an oxidizing agent of sulfides. Furthermore, the activity of acidophilic Fe-oxidizing bacteria is favored below pH 3, and, therefore, the regeneration of Fe(III) could be produced. Anyway, although this experiment was not performed under sterile conditions, their involvement in such process should be much lesser than under natural conditions. On the other hand, the solubility of scorodite increases greatly below pH 2 [23], and, consequently, the release of As, whereas above this pH value the gradual transformation of AFA into hydrous ferric oxides implies the progressive stabilization of As. A similar process occurs with jarosite minerals at pH values close to 3 [87].

4. CONCLUSIONS

The characterization of sulfidic mine wastes comprising important amounts of arsenopyrite along with pyrite/marcasite revealed the occurrence of scorodite, AFA, elemental sulfur, hydronium jarosite, goethite, hematite and hydrous ferric oxides as the main weathering products. The hardpan mainly consisted of arsenopyrite (partially or completely altered), pyrite/marcasite and grains of other gangue minerals (quartz, mica and feldspar), cemented by a yellowish phase of cracked texture. This phase corresponded to AFA together with elemental sulfur, and was also the binding material occurring in the other cemented phases. Hydronium jarosite and Fe (oxyhydr)oxides were enriched in As, with values of 0.19-3.98 and 0.81-7.49 wt.% As_2O_5, respectively. AFA presented Fe/As molar ratios comprised within the range 1.14-1.85. Accordingly, the hardpan and cemented phases accumulated high As levels (up to 7.9%). Nevertheless, their As leachability and lability were not decreased with respect to those of weathered phases not showing cementation in the mine wastes. Moreover, their leachable As contents make them to be classified as wastes not acceptable at landfills for hazardous wastes unless a treatment was applied to reduce such contents down to 25 mg kg^{-1}. The different weathered phases presented pH values characteristic of acid producing materials, pointing out that the alteration of sulfide minerals was still progressing. Such conditions allowed the occurrence of different secondary products such as hydronium jarosite, scorodite and AFA. Therefore, the stability of the hardpan and cemented phases could be compromised as sulfides became consumed. Nevertheless, at higher pH levels ($\geq$ 4), especially when circumneutral conditions dominate, the release of As from mine wastes decreased drastically, with this As

abatement being likely caused by the precipitation and scavenging action of Fe (oxyhydr)oxides.

ACKNOWLEDGMENTS

The financial support to perform this study was provided by the Spanish Mining Company Saloro SLU (contract numbers: article 83-18LB0Ñ and 080102130007), which is greatly acknowledged.

REFERENCES

[1] B.G. Lottermoser, Mine Wastes-Characterization, Treatment and Environmental Impacts, third ed., Springer, Heidelberg, 2010.

[2] L. Alakangas, B. Öhlander, Formation and composition of cemented layers in low-sulphide mine tailings, Laver, northern Sweden, Environ. Geol. 50 (2006) 809-819.

[3] S.L. DeSisto, H.E. Jamieson, M.B. Parsons, Influence of hardpan layers on arsenic mobility in historical gold mine tailings, Appl. Geochem. 26 (2011) 2004-2018.

[4] T. Graupner, A. Kassahun, D. Rammlmair, J.A. Meima, D. Kock, M. Furche, A. Fiege, A. Schippers, F. Melcher, Formation of sequences of cemented layers and hardpans within sulfide-bearing mine tailings (mine district Freiberg, Germany), Appl. Geochem. 22 (2007) 2486-2508.

[5] M. Redwan, D. Rammlmair, Influence of climate, mineralogy and mineral processing on the weathering behaviour within two, low-sulfide, high-carbonate, gold mine tailings in the Eastern Desert of Egypt, Environ. Earth Sci. 65 (2012) 2179-2193.

[6] M.C. Moncur, C.J. Ptacek, D.W. Blowes, J.L. Jambor, 2005. Release, transport and attenuation of metals from an old tailings impoundment, Appl. Geochem. 20 (2005) 639-659.

[7] N.V. Sidenko, E.V. Lazareva, S.B. Bortnikova, A.D. Kireev, B.L. Sherriff, Geochemical and mineralogical zoning of high-sulfide mine-waste at the Berikul mine-site, Kemerovo region, Russia, Can. Mineral. 43 (2005) 1141-1156.

[8] A. Xenidis, E. Mylona, A.D. Harokopou, Enhancement of hardpan formation by amending sulphidic tailings with limestone or fly ash, Land Contam. Recl. 15 (2007) 359-373.

[9] D. Quispe, R. Pérez-López, P. Acero, C. Ayora, J.M. Nieto, R. Tucoulou, Formation of a hardpan in the co-disposal of fly ash and sulfide mine tailings and its influence on the generation of acid mine drainage, Chem. Geol. 355 (2013) 45-55.

[10] R.G. McGregor, D.W. Blowes, The physical, chemical and mineralogical properties of three cemented layers within sulfide-bearing mine tailings, J. Geochem. Explor. 76 (2002) 195-207.

[11] M. Redwan, D. Rammlmair, J.A. Meima, Application of mineral liberation analysis in studying micro-sedimentological structures within sulfide mine tailings and their effect on hardpan formation, Sci. Total Environ. 414 (2012) 480-493.

[12] M.B.J. Lindsay, M.C. Moncur, J.G. Bain, J.L. Jambor, C.J. Ptacek, D.W. Blowes, Geochemical and mineralogical aspects of sulfide mine tailings, Appl. Geochem. 57 (2015) 157-177.

[13] B.G. Lottermoser, P.M. Ashley, Mobility and retention of trace elements in hardpan-cemented cassiterite tailings, north Queensland, Australia, Environ. Geol. 50 (2006) 835-846.

[14] R. Hakkou, M. Benzaazoua, B. Bussière, Acid mine drainage at the abandoned kettara mine (Morocco): 2. mine waste geochemical behavior, Mine Water Environ. 27 (2008) 160-170.

[15] C. Carbone, E. Dinelli, P. Marescotti, G. Gasparotto, G. Lucchetti, The role of AMD secondary minerals in controlling environmental pollution: Indications from bulk leaching tests, J. Geochem. Explor. 132 (2013) 188-200.

[16] P.M. Ashley, B.G. Lottermoser, A.J. Collins, C.D. Grant, Environmental geochemistry of the derelict Webbs Consols mine, New South Wales, Australia, Environ. Geol. 46 (2004) 591-604.

[17] R. Gieré, N.V. Sidenko, E.V. Lazareva, The role of secondary minerals in controlling the migration of arsenic and metals from high-sulfide wastes (Berikul gold mine, Siberia), Appl. Geochem. 18 (2003) 1347-1359.

[18] C.L. Corkhill, P.L. Wincott, J.R. Lloyd, D.J. Vaughan, The oxidative dissolution of arsenopyrite (FeAsS) and enargite (Cu_3AsS_4) by *Leptospirillum ferrooxidans*, Geochim. Cosmochim. Acta 72 (2008) 5616-5633.

[19] M.A. McKibben, B.A. Tallant, J.K. del Angel, Kinetics of inorganic arsenopyrite oxidation in acidic aqueous solutions, Appl. Geochem. 23 (2008) 121-135.

[20] C.L. Corkhill, D.J. Vaughan, Arsenopyrite oxidation - A review, Appl. Geochem. 24 (2009) 2342-2361.

[21] P. Drahota, M. Filippi, Secondary arsenic minerals in the environment: A review, Environ. Int. 35 (2009) 1243-1255.

[22] M.P. Asta, J. Cama, C. Ayora, P. Acero, G. de Giudici, Arsenopyrite dissolution rates in O_2-bearing solutions, Chem. Geol. 273 (2010) 272-285.

[23] D. Paktunc, K. Bruggeman, Solubility of nanocrystalline scorodite and amorphous ferric arsenate: Implications for stabilization of arsenic in mine wastes, Appl. Geochem. 25 (2010) 674-683.

[24] A. Murciego, E. Álvarez-Ayuso, E. Pellitero, M.A. Rodríguez, A. García-Sánchez, A. Tamayo, F. Rubio, J. Rubin, Study of arsenopyrite weathering products in mine wastes from abandoned tungsten and tin exploitations, J. Hazard. Mater. 186 (2011) 590-601.

[25] M. Filippi, P. Drahota, V. Machovič, V. Böhmová, M. Mihaljevič, Arsenic mineralogy and mobility in the arsenic-rich historical mine waste dump, Sci. Total Environ. 536 (2015) 713-728.

[26] P. Drahota, M. Knappová, H. Kindlová, A. Culka, J. Majzlan, M. Mihaljevič, J. Rohovec, F. Veselovský, M. Fridrichová, J. Jehlička, Mobility and attenuation of arsenic in sulfide-rich mining wastes from the Czech Republic, Sci. Total Environ. 557-558 (2016) 192-203.

[27] N.E. Nieva, L. Borgnino, F. Locati, M.G. García, Mineralogical control on arsenic release during sediment-water interaction in abandoned mine wastes from the Argentina Puna, Sci. Total Environ. 550 (2016) 1141-1151.

[28] J.C.M. Silva, E.C. Dos Santos, T. Heine, H.A. De Abreu, H.A. Duarte, Oxidation Mechanism of Arsenopyrite in the Presence of Water, J. Phys. Chem. C 121 (2017) 26887-26894.

[29] O. Sracek, M. Mihaljevic, B. Kríbek, V. Majer, J. Filip, A. Vanek, V. Penížek, V. Ettler, B. Mapani, Geochemistry of mine tailings and behavior of arsenic at Kombat, northeastern Namibia, Environ. Monit. Assess. 186 (2014) 4891-4903.

[30] H.W. Nesbitt, I.J. Muir, A.R. Pratt, Oxidation of arsenopyrite by air and air saturated, distilled water and implications for mechanisms of oxidation, Geochim. Cosmochim. Acta 59 (1995) 1773-1786.

[31] A. Carrillo-Chávez, E. Salas-Megchún, G. Levresse, C. Muñoz-Torres, O. Pérez-Arvizu, T. Gerke, Geochemistry and mineralogy of mine-waste material from a “skarn-type” deposit in central Mexico: Modeling geochemical controls of metals in the surface environment, J. Geochem. Explor. 144 (2014) 28-36.

[32] M. M. Salvarredy-Aranguren, A. Probst, M. Roulet , M.-P. Isaure, Contamination of surface waters by mining wastes in the Milluni Valley (Cordillera Real, Bolivia): Mineralogical and hydrological influences, Appl. Geochem. 23 (2008) 1299-1324.

[33] S. P. Lopes, M.M.V.G. Silva, E.M.C. Gomes, P.C.S. Carvalho, A.M.R. Neiva, Seasonal contamination of surface waters close to an abandoned Sn-W mine, northeast Portugal, Environ. Earth Sci. 75 (2016) 1438.

[34] L. Haffert, D. Craw, J. Pope, Climatic and compositional controls on secondary arsenic mineral formation in high-arsenic mine wastes, South Island, New Zealand, New Zeal. J. Geol. Geop. 53 (2010) 91-101.

[35] A. Parviainen, M.B.J. Lindsay, R. Pérez-López, B.D. Gibson, C.J. Ptacek, D.W. Blowes, K. Loukola-Ruskeeniemi, Arsenic attenuation in tailings at a former Cu–W–As mine, SW Finland, Appl. Geochem. 27 (2012) 2289-2299.

[36] L. Haffert, D. Craw, Geochemical processes influencing arsenic mobility at Bullendale historic gold mine, Otago, New Zealand, New Zealand, New Zeal. J. Geol. Geop. 53 (2010) 129-142.

[37] M. Filippi, V. Machovič, P. Drahota, V. Böhmová, Raman microspectroscopy as a valuable additional method to x-ray diffraction and electron microscope/microprobe analysis in the study of iron arsenates in environmental samples, Appl. Spectrosc. 63 (2009) 621-626.

[38] H. Jelenová, J. Majzlan, F.Y. Amoako, P. Drahota, Geochemical and mineralogical characterization of the arsenic-, iron-, and sulfur-rich mining waste dumps near Kaňk, Czech Republic, Appl. Geochem. 97 (2018) 247-255.

[39] S.R. Walker, M.B. Parsons, H.E. Jamieson, A. Lanzirotti, Arsenic mineralogy of near-surface tailings and soils: Influences on arsenic mobility and bioaccessibility in the Nova Scotia gold mining districts, Can. Mineral. 47 (2009) 533-556.

[40] D. Paktunc, 2015, Phase transformations in the system Fe-AsO_4-SO_4 and the structure of amorphous ferric arsenate: Implications for arsenic stabilization in mine drainage and industrial effluents, Can. Mineral. 53 (2015) 921-936.

[41] D. Paktunc, J. Dutrizac, V. Gertsman, Synthesis and phase transformations involving scorodite, ferric arsenate and arsenical ferrihydrite: Implications for arsenic mobility, Geochim. Cosmochim. Acta 72 (2008) 2649-2672.

[42] D. Paktunc, J. Majzlan, A. Huang, Y. Thibault, M.B. Johnson, M.A. White, Synthesis, characterization, and thermodynamics of arsenates forming in the Ca-Fe(III)-As(V)-NO_3 system: Implications for the stability of Ca-Fe arsenates, Am. Mineral. 100 (2015) 1803-1820.

[43] P. Drahota, O. Kulakowski, A. Culka, M. Knappová, J. Rohovec, F. Veselovský, M. Racek, Arsenic mineralogy of near-neutral soils and mining waste at the Smolotely-Líšnice historical gold district, Czech Republic, Appl. Geochem. 89 (2018) 243-254.

[44] M. Filippi, V. Goliáš, Z. Pertold, Arsenic in contaminated soils and anthropogenic deposits at the Mokrsko, Roudný, and Kašperské Hory gold deposits, Bohemian Massif (CZ), Environ. Geol. 45 (2004) 716-730.

[45] P. Drahota, J. Rohovec, M. Filippi, M. Mihaljevič, P. Rychlovský, V. Cervený, Z. Pertold, Mineralogical and geochemical controls on arsenic speciation and mobility under different redox conditions in soil, sediment and water at the Mokrsko-West gold deposit, Czech Republic. Sci. Total Environ. 407 (2009) 3372-3384.

[46] M. Márquez, J. Gaspar, K.E. Bessler, G. Magela, Process mineralogy of bacterial oxidized gold ore in São Bento Mine (Brasil), Hydrometallurgy 83 (2006) 114-123.

[47] D. Mains, D. Craw, Composition and mineralogy of historic gold processing residues, east Otago, New Zealand, New Zeal. J. Geol. Geop. 48 (2005) 641-647.

[48] R. Siuda, Supergene parageneses of the Radzimowice deposit (Kaczawa Mts., Poland) [Paragenezy hipergeniczne ztoża Radzimowice (Góry Kaczawskie)] Przeglad Geologiczny 60 (2012) 442-449.

[49] F. Frau, C. Ardau, L. Fanfani, Environmental geochemistry and mineralogy of lead at the old mine area of Baccu Locci (south-east Sardinia, Italy), J. Geochem. Explor. 100 (2009) 105-115.

[50] E. Kocourková-Víšková, J. Loun, O. Sracek, S. Houzar, J. Filip, Secondary arsenic minerals and arsenic mobility in a historical waste rock pile at Kaňk near Kutná Hora, Czech Republic, Miner. Petrol. 109 (2015) 17-33.

[51] F.M. Romero, M.A. Armienta, G. Villaseñor, J.L. González, Mineralogical constraints on the mobility of arsenic in tailings from Zimapán, Hidalgo, Mexico, IJEP 26 (2006) 23-40.

[52] E. Kocourková, O. Sracek, S. Houzar, J. Cempírek, Z. Losos, J. Filip, P. Hršelová, Geochemical and mineralogical control on the mobility of arsenic in a waste rock pile at Dlouhá Ves, Czech Republic, J. Geochem. Explor. 110 (2011) 61-73.

[53] A. Schippers, A.A. Nagy, D. Kock, F. Melcher, E.-D. Gock, The use of FISH and real-time PCR to monitor the biooxidation and cyanidation for gold and silver recovery from a mine tailings concentrate (Ticapampa, Peru), Hydrometallurgy 94 (2008) 77-81.

[54] R.A. Jones, S.F. Koval, H.W. Nesbitt, Surface alteration of arsenopyrite (FeAsS) by *Thiobacillus ferrooxidans*, Geochim. Cosmochim. Acta 67 (2003) 955-965.

[55] Y. Yunmei, Z. Yongxuan, A.E. Williams-Jones, G. Zhenmin, L. Dexian, A kinetic study of the oxidation of arsenopyrite in acidic solutions: implications for the environment, Appl. Geochem. 19 (2004) 435-444.

[56] M.G.M. Fernandez, C. Mustin, P. de Donato, O. Barres, P. Marion, J. Berthelin, Occurrences at mineral-bacterial interface during oxidation of arsenopyrite by *Thiobacillus ferrooxidans*, Biotechnol. Bioeng. 46 (1995) 13-21.

[57] M.I. Sampson, C.V. Philips, A.S. Ball, Investigation of the attachment of *Thiobacillus ferrooxidans* to mineral surfaces using scanning electron microscopy analysis, Miner. Eng. 13 (2000) 643-656.

[58] C. Streten-Joyce, J. Manning, K.S. Gibb, B.A. Neilan, D.L. Parry, The chemical composition and bacteria communities in acid and metalliferous drainage from the wet–dry tropics are dependent on season, Sci. Total Environ. 443 (2013) 65-79.

[59] P.L. Bond, G.K. Druschel, J.F. Banfield, Comparison of acid mine drainage microbial communities in physically and geochemically distinct ecosystems, Appl. Environ. Microbiol. 66 (2000) 4962-71.

[60] B.J. Baker, J.F. Banfield, Microbial communities in acid mine drainage, FEMS Microb. Ecol. 44 (2003) 139-152.

[61] K.J. Edwards, T.M. Gihring, J.F. Banfield, Seasonal variations in microbial populations and environmental conditions in an extreme acid mine drainage environment, Appl. Environ. Microbiol. 65 (1999) 3627-3632.

[62] EN-12457-4, Characterization of Waste - Leaching-Compliance Test for Leaching of Granular Waste Materials and Sludges - Part 4: One Stage Batch Test at a Liquid to Solid Ratio of 10 l/kg for Materials with Particle Size below 10 mm (without or with Size Reduction), European Committee for Standardization, Brussels, 2002.

[63] W.W. Wenzel, N. Kirchbaumer, T. Prohaska, G. Stingeder, E. Lombi, D.C. Adriano, Arsenic fractionation in soils using an improved sequential extraction procedure, Anal. Chim. Acta 436 (2001) 309-323.

[64] D. Baron, C.D. Palmer, Solubility of jarosite at 4-35°C, Geochim. Cosmochim. Acta 60 (1996) 185-195.

[65] B. Gasharova, J. Göttlicher, U. Becker, Dissolution at the surface of jarosite: An in situ AFM study, Chem. Geol. 215 (2005) 499-516.

[66] K.S. Savage, D.K. Bird, P.A. O'Day, Arsenic speciation in synthetic jarosite, Chem. Geol. 215 (2005) 473-498.

[67] I. Ko, A.P. Davis, J.-Y. Kim, K.-W. Kim, Effect of contact order on the adsorption of inorganic arsenic species onto hematite in the presence of humic acid, J. Hazard. Mater. 141 (2007) 53-60.

[68] M.P. Asta, J. Cama, M. Martínez, J. Giménez, Arsenic removal by goethite and jarosite in acidic conditions and its environmental implications, J. Hazard. Mater. 171 (2009) 965-972.

[69] M. Zhang, M. Dai, L. Xia, S. Song, Comparison of arsenic adsorption on goethite and amorphous ferric oxyhydroxide in water, Water Air Soil Poll. 228 (2017) 427.

[70] S. Das, M.J. Hendry, Application of Raman spectroscopy to identify iron minerals commonly found in mine wastes, Chem. Geol. 290 (2011) 101-108.

[71] A. Courtin-Nomade, H. Bril, J.-M. Bény, M. Kunz, N. Tamura, Sulfide oxidation observed using micro-Raman spectroscopy and micro-X-ray diffraction: The importance of water/rock ratios and pH conditions, Am. Miner. 95 (2010) 582-591.

[72] A.I. Apopei, N. Buzgar, G. Damian, A. Buzatu, The Raman study of weathering minerals from the Coranda-Hondol open pit (Certej gold-silver deposit) and their photochemical degradation products under laser irradiation, Can. Mineral. 52 (2014) 1027-1038.

[73] P. Makreski, J. Todorov, V. Makrievski, L. Pejov, G. Jovanovski, Vibrational spectra of the rare-occurring complex hydrogen arsenate minerals pharmacolite, picropharmacolite, and vladimirite: Dominance of Raman over IR spectroscopy to discriminate arsenate and hydrogen arsenate units, J. Raman Spectrosc. 49 (2018) 747-763.

[74] D.L.A. de Faria, S. Venâncio Silva, M.T. de Oliveira, Raman microspectroscopy of some iron oxides and oxyhydroxides, J. Raman Spectrosc. 28 (1997) 873-878.

[75] M. Hanesch, Raman spectroscopy of iron oxides and (oxy)hydroxides at lower laser power and possible applications in environmental magnetic studies, Geophys. J. Int. 177 (2009) 941-948.

[76] Y. Jia, L. Xu, Z. Fang, G.P. Demopoulos, 2006, Observation of surface precipitation of arsenate on ferrihydrite, Environ. Sci. Technol. 40 (2006) 3248-3253.

[77] K. Müller, V.S.T. Ciminelli, M.S.S. Dantas, S. Willscher, A comparative study of As(III) and As(V) in aqueous solutions and adsorbed on iron oxy-hydroxides by Raman spectroscopy, Water Res. 44 (2010) 5660-5672.

[78] M. Filippi, Oxidation of the arsenic-rich concentrate at the Přebuz abandoned mine (Erzgebirge Mts., CZ): mineralogical evolution, Sci. Total Environ. 322 (2004) 271-282.

[79] H.W. Nesbitt, I.J. Muir, Oxidation states and speciation of secondary products on pyrite and arsenopyrite reacted with mine waste waters and air, Mineral. Petrol. 62 (1998) 123-144.

[80] A. Basu, M.E. Schreiber, Arsenic release from arsenopyrite weathering: Insights from sequential extraction and microscopic studies, J. Hazard. Mater. 262 (2013) 896-904.

[81] M.M. McGuire, K.J. Edwards, J.F. Banfield, R.J. Hamers, Kinetics, surface chemistry, and structural evolution of microbially mediated sulfide mineral dissolution, Geochim. Cosmochim. Acta 65 (2001) 1243-1258.

[82] L. Haffert, D. Craw, Field quantification and characterisation of extreme arsenic concentrations at a historic mine processing site, Waiuta, New Zealand, New Zeal. J. Geol. Geop. 52 (2009) 261-272.

[83] L. Haffert, D. Craw, Mineralogical controls on environmental mobility of arsenic from historic mine processing residues, New Zealand, Appl.Geochem. 23 (2008) 1467-1483.

[84] R.A. Root, S.M. Hayes, C.M. Hammond, R.M. Maier, J. Chorover, Toxic metal(loid) speciation during weathering of iron sulfide minetailings under semi-arid climate, Appl. Geochem. 62 (2015) 131-149.

[85] K.A. Hudson-Edwards, C. Schell, M.G. Macklin, Mineralogy and geochemistry of alluvium contaminated by metal mining in the Rio Tinto area, southwest Spain, Appl. Geochem. 14 (1999) 1015-1030.

[86] A. Zdravković, V. Cvetković, A. Pačevski, A. Rosić, K. Šarić, V. Matović, S. Erić, Products of oxidative dissolution on waste rock dumps at the Pb-Zn Rudnik mine in Serbia and their possible effects on the environment, J. Geochem. Explor. 181 (2017) 160-171.

[87] S.A. Welch, D. Kirste, A.G. Christy, F.R. Beavis, S.G. Beavis, Jarosite dissolution II-Reaction kinetics, stoichiometry and acid flux, Chem. Geol. 254 (2008) 73-86.

[88] J. Sánchez-España, I. Yusta, G.A. López, Schwertmannite to jarosite conversión in the water column of an acidic mine pit lake, Mineral. Mag. 76 (2012) 2659-2682.

[89] P. Acero, C. Ayora, C. Torrentó, J.-M. Nieto, The behavior of trace elements during schwertmannite precipitation and subsequent transformation into goethite and jarosite. Geochim. Cosmochim. Acta 70 (2006) 4130-4139.

[90] H. Wang, J.M. Bigham, O.H. Tuovinen, Formation of schwertmannite and its transformation to jarosite in the presence of acidophilic iron-oxidizing microorganisms, Mat. Sci. Eng. C 26 (2006) 588-592.

[91] L. Carlson, J.M. Bigham, U. Schwertmann, A. Kyek, F. Wagner, Scavenging of As from acid mine drainage by schwertmannite and ferrihydrite: A comparison with synthetic analogues, Environ. Sci. Technol. 36 (2002) 1712-1719.

[92] F. Maillot, G. Morin, F. Juillot, O. Bruneel, C. Casiot, G. Ona-Nguema, Y. Wang, S. Lebrun, E. Aubry, G. Vlaic, G.E. Brown, Structure and reactivity of As(III)- and As(V)-rich schwertmannites and amorphous ferric arsenate sulfate from the Carnoulès acid mine drainage, France: Comparison with biotic and abiotic model compounds and implications for As remediation, Geochim. Cosmochim. Acta 104 (2013) 310-329.

[93] Council Decision 2003/33/EC of 19 December 2002 establishing criteria and procedures for the acceptance of waste at landfills pursuant to Article 16 of and Annex II to Directive 1999/31/EC, Off J Eur Commun L11 (2002) 27-49.

[94] E. Moreno-Jiménez, R. Manzano, E. Esteban, J. Peñalosa, The fate of arsenic in soils adjacent to an old mine site (Bustarviejo, Spain): Mobility and transfer to native flora, J. Soils Sediments 10 (2010) 301-312.

[95] S. Wang, C.N. Mulligan, Speciation and surface structure of inorganic arsenic in solid phases: A review, Environ. Int. 34 (2008) 867-879.

[96] C.C. Fuller, J.A. Dadis, G.A. Waychunas, Surface chemistry of ferrihydrite: Part 2. Kinetics of arsenate adsorption and coprecipitation, Geochim. Cosmochim. Acta 57 (1993) 2271-2282.

[97] B.J. Moldovan, D.T. Jiang, M.J. Hendry, Mineralogical characterization of arsenic in uranium mine tailings precipitated from iron-rich hydrometallurgical solutions, Environ. Sci. Technol. 37 (2003) 873-879.

[98] E. Krause, V.A. Ettel, Solubilities and stabilities of ferric arsenate compounds, Hydrometallurgy 22 (1989) 311-337.

Table 1. Spot chemical analyses of sulfide weathering products.

Composition (%)	Sc (n =22)	CYPh (n = 41)	Jar (n = 10)	Gth (n = 10)	Hem (n =7)	CRPh (n = 31)
Fe_2O_3	35.42 (31.07-37.23)	38.46 (32.46-50.46)	44.21 (41.20-45.45)	76.86 (73.84-79.84)	86.38 (83.54-88.58)	71.71 (50.80-78.84)
As_2O_5	47.63 (42.24-49.65)	39.49 (29.41-48.29)	0.91 (0.19-3.98)	2.23 (1.30-2.81)	1.32 (0.81-2.11)	5.84 (3.95-7.49)
SO_3	1.03 (0.59-4.45)	7.36 (1.36-22.11)	33.29 (29.83-35.24)	< l.d.-2.42	0.36 (0.17-1.05)	< l.d.-7.58
P_2O_5	< l. d-0.05	< l.d.-2.76	< l.d.-0.05	0.72 (0.60-1.16)	0.54 (0.34-0.78)	1.30 (0.84-1.85)
MnO	< l. d-0.07	< l.d.-0.07	< l.d.-0.02	< l.d.-0.12	< l.d.-0.03	< l.d.-0.16
Na_2O	< l. d-0.05	< l.d.-1.02	0.86 (060-1.12)	< l.d.-0.08	< l.d.-0.05	< l.d.-0.85
SiO_2	< l. d-0.06	< l.d.-6.28	1.57 (0.43-4.75)	1.67 (0.71-3.02)	3.62 (3.04-3.97)	1.38 (0.22-7.68)
K_2O	< l. d-0.02	< l.d.-0.11	0.70 (0.27-0.96)	< l.d.-0.05	< l.d.-0.01	< l.d.-0.62
Al_2O_3	< l. d	< l.d.-2.45	0.30 (0.08-1.02)	1.72 (0.01-4.18)	< l.d.-0.09	2.51 (1.13-6.79)

Sc: Scorodite, CYPh: cracked yellow phases, Jar: jarosite group minerals, Gth: goethite, Hem: hematite, CRPh: cracked red phases.

Table 2. Environmental parameters of the different types of mine waste samples. (Different letters (a-e) within values of the same environmental parameter mean significant differences at $p < 0.05$, evaluated by the Student's t-test).

	Py/Mrc and WP	Apy and WP	Cemented phases	Hardpan	Upper zone (hardpan)	Bottom zone (hardpan)
pH	3.1 ± 0.1 ^{a}	2.6 ± 0.1 ^{b}	3.4 ± 0.1 ^{c}	3.1 ± 0.1 ^{a}	3.2 ± 0.1 ^{a}	3.1 ± 0.1 ^{a}
Total As (%)	5.03 ± 0.30 ^{a}	25.6 ± 3.7 ^{b}	6.35 ± 0.83 ^{c}	7.93 ± 0.79 ^{d}	10.4 ± 1.2 ^{e}	7.04 ± 0.29 ^{acd}
Leachable As (mg kg^{-1})	14.5 ± 0.9 ^{a}	76.7 ± 4.6 ^{b}	28.0 ± 0.8 ^{c}	39.6 ± 4.4 ^{cd}	59.1 ± 4.4 ^{bd}	21.8 ± 1.7 ^{c}
Labile As(mg kg^{-1})	17.8 ± 1.1 ^{a}	220 ± 3 ^{b}	186 ± 19 ^{bd}	96.3 ± 5.9 ^{c}	210 ± 1 ^{d}	76.2 ± 1.5 ^{e}
Toxicity (As (mg L^{-1}))	0.50 ± 0.01 ^{a}	6.3 ± 1.2 ^{b}	2.4 ± 0.3 ^{c}	3.0 ± 0.4 ^{d}	4.4 ± 0.8 ^{e}	2.0 ± 0.1 ^{c}

Py: Pyrite, Mrc: marcasite, WP: weathering products, Apy: arsenopyrite.

Table 3. Contents of As released from the various types of mine waste samples at different pH values. (Different letters (a-d) within pH values of the same type of mine waste sample mean significant differences at $p < 0.05$, evaluated by the Student's t-test).

pH	Py/Mrc and WP	Apy and WP	Cemented phases	Hardpan	Upper zone (hardpan)	Bottom zone (hardpan)
	As (mg kg^{-1})					
1	1923 ± 65 [a]	5890 ± 568 [a]	11375 ± 292 [a]	10312 ± 178 [a]	13027 ± 29 [a]	11228 ± 764 [a]
2	449 ± 40 [b]	2154 ± 156 [b]	1398 ± 48 [b]	888 ± 25 [b]	1914 ± 37 [b]	784 ± 83 [b]
4	91.4 ± 11.5 [c]	667 ± 13 [c]	135 ± 11 [c]	73.7 ± 3.2 [c]	145 ± 4 [c]	62.2 ± 0.9 [c]
6	9.2 ± 2.1 [d]	417 ± 8 [d]	75.4 ± 9.0 [d]	52.7 ± 1.9 [d]	103 ± 1 [d]	44.2± 2.4 [d]
8	7.5 ± 3.0 [d]	452 ± 12 [d]	65.0 ± 8.0 [d]	53.0 ± 1.8 [d]	99.2 ± 2.4 [d]	45.6 ± 1.2 [d]

Py: Pyrite, Mrc: marcasite, WP: weathering products, Apy: arsenopyrite.

Figure captions

Figure 1. Images of hand samples: hardpan fragments (a), arsenopyrite weathered to scorodite (b), weathered pyrite/marcasite (c), fragment of gangue minerals with cemented phases (d), and cemented phases (e) (Apy: arsenopyrite, Cm: cementing material, CPh: cemented phases, Mrc: marcasite, Ms: muscovite, Py: pyrite, Q: quartz, Sc: scorodite, WP: weathering products).

Figure 2. Representative XRD patterns of mine waste samples: weathered sulfides (A, B and C), cemented phases (D), hardpan (E) and ore minerals (F) (Ab: albite, Apy: arsenopyrite, Gth: goethite, Hem: hematite, HJ: hydronium jarosite, Mrc: marcasite, Ms: muscovite, Py: pyrite, Q: quartz, S: elemental sulfur, Sc: scorodite, Sch: scheelite, Wo: wolframite).

Figure 3. Microscopy images of weathered sulfides: arsenopyrite altered to microcrystalline scorodite (a and b), pyrite weathered to cracked red phases (c and d), pyrite weathered to goethite and hematite (e and f), marcasite altered to jarosite-group minerals (g, h and i) (transmitted light-x40-uncrossed polarizers: a, c, e and g, reflected light-x40-uncrossed polarizers: b, d, f and h (x100: yellow box in f), transmitted light-x40-crossed polarizers: i) (Apy: arsenopyrite, CRPh: cracked red phases, Fe Ox: Fe (oxyhydr)oxides Gth: goethite, Hem: hematite, Jar: jarosite-group minerals, Mrc: marcasite, Py: pyrite, Sc: scorodite).

Figure 4. Microscopy and electron backscatter images of cemented phases (a, b and g) and hardpan (c, d, e, f and h) (transmitted light-x40-uncrossed polarizers: a and c (x100: red box in a), transmitted light-x40-crossed polarizers: b and d, transmitted light-x100-uncrossed polarizers: e, reflected light-x100-uncrossed polarizers: f, electron backscatter images: g and h) (Apy: arsenopyrite, Cm: cementing material, CYPh: cracked yellow phases, Fd: feldspar, Ms: muscovite, Py: pyrite, Q: quartz).

Figure 5. Representative micro-Raman spectra of sulfide weathering products (Sc: Scorodite, CYPh: cracked yellow phases, Jar: jarosite-group minerals, Gth: goethite, Hem: hematite).

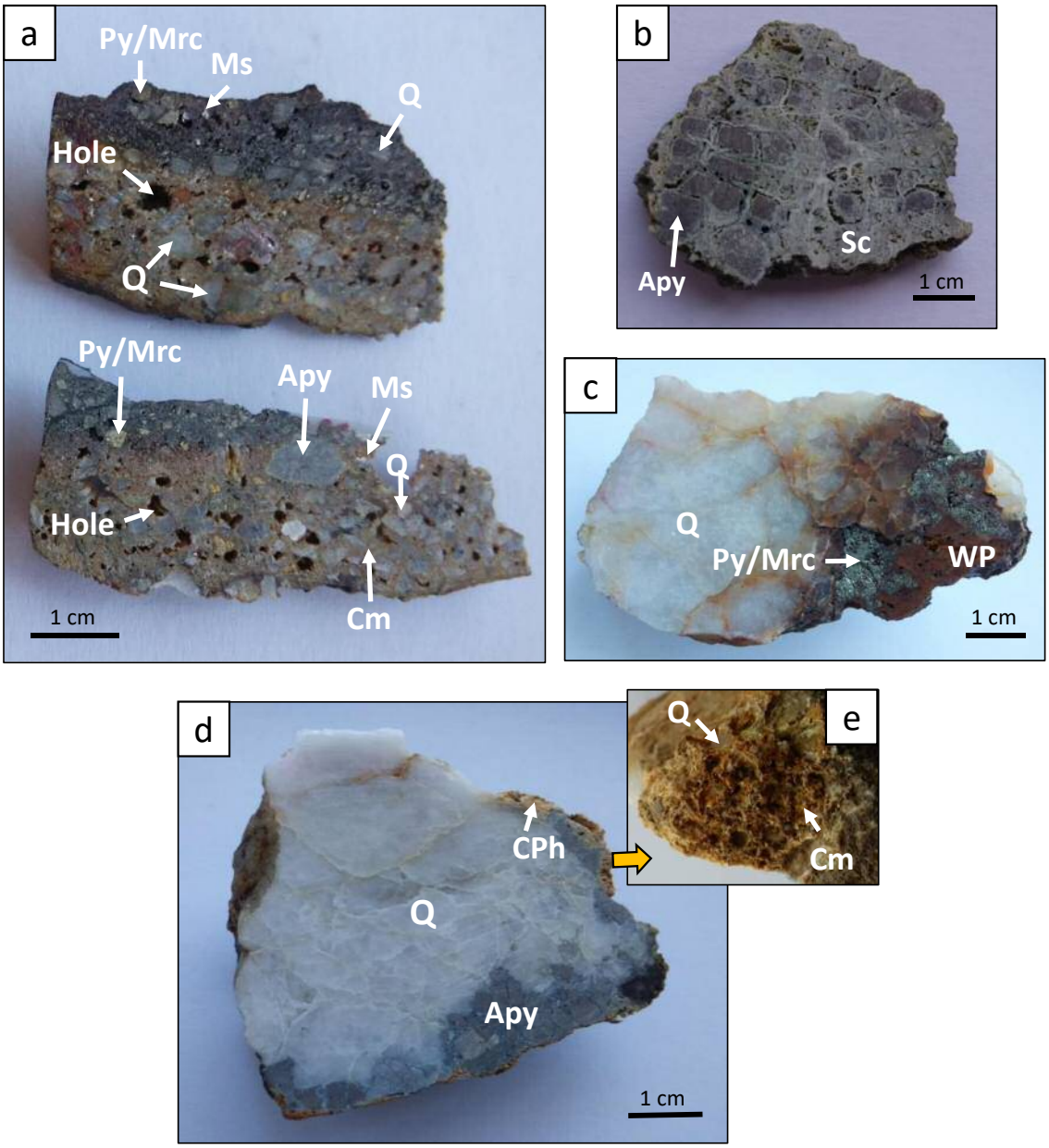
a
Py/Mrc
Ms
Q
Hole
Q
Py/Mrc
Apy
Ms
Q
Hole
1 cm
Cm
b
Apy
Sc
1 cm
c
Q
Py/Mrc
WP
1 cm
d
CPh
Q
Apy
1 cm
e
Q
Cm

Figure 1.

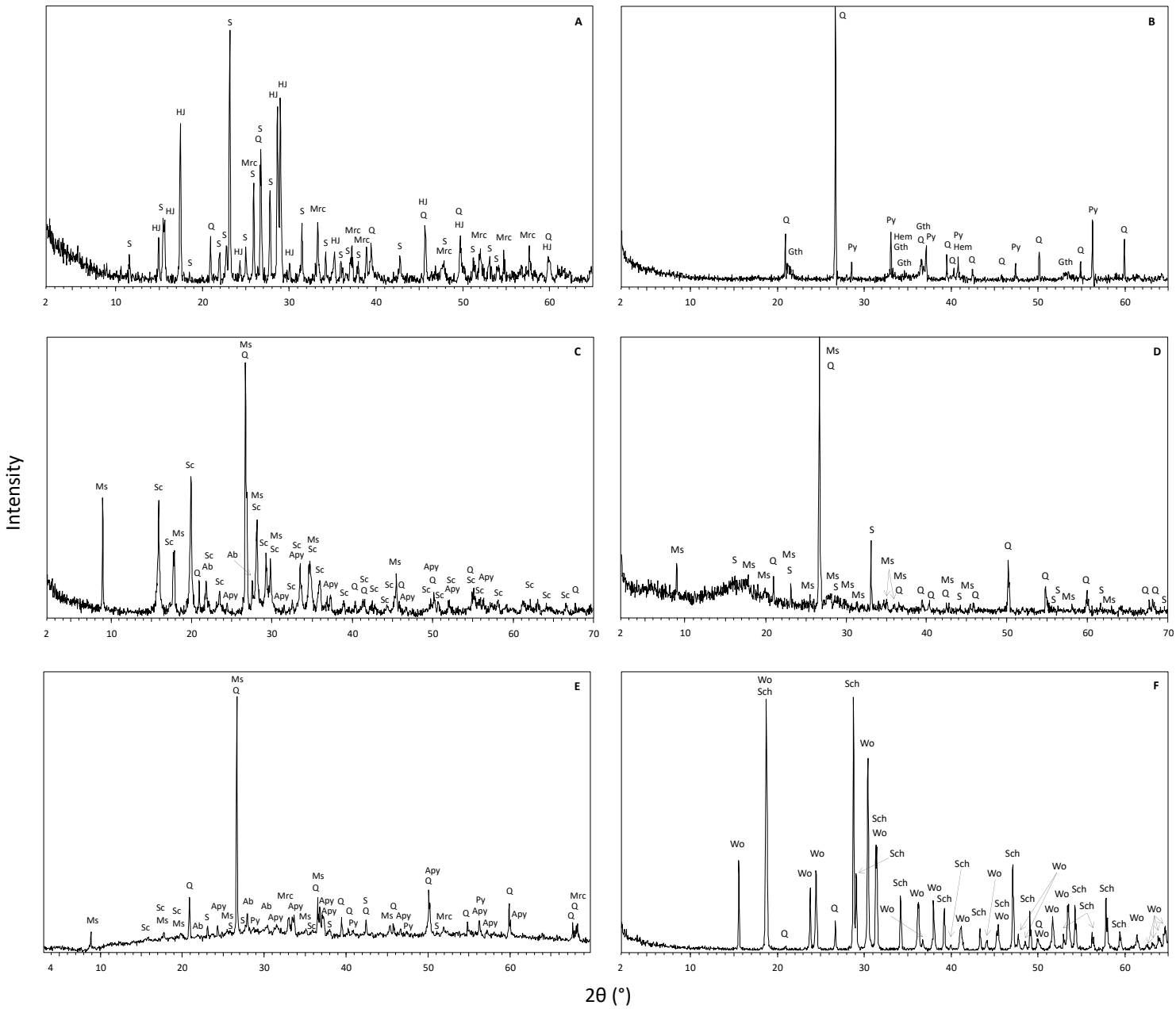

Figure 2.

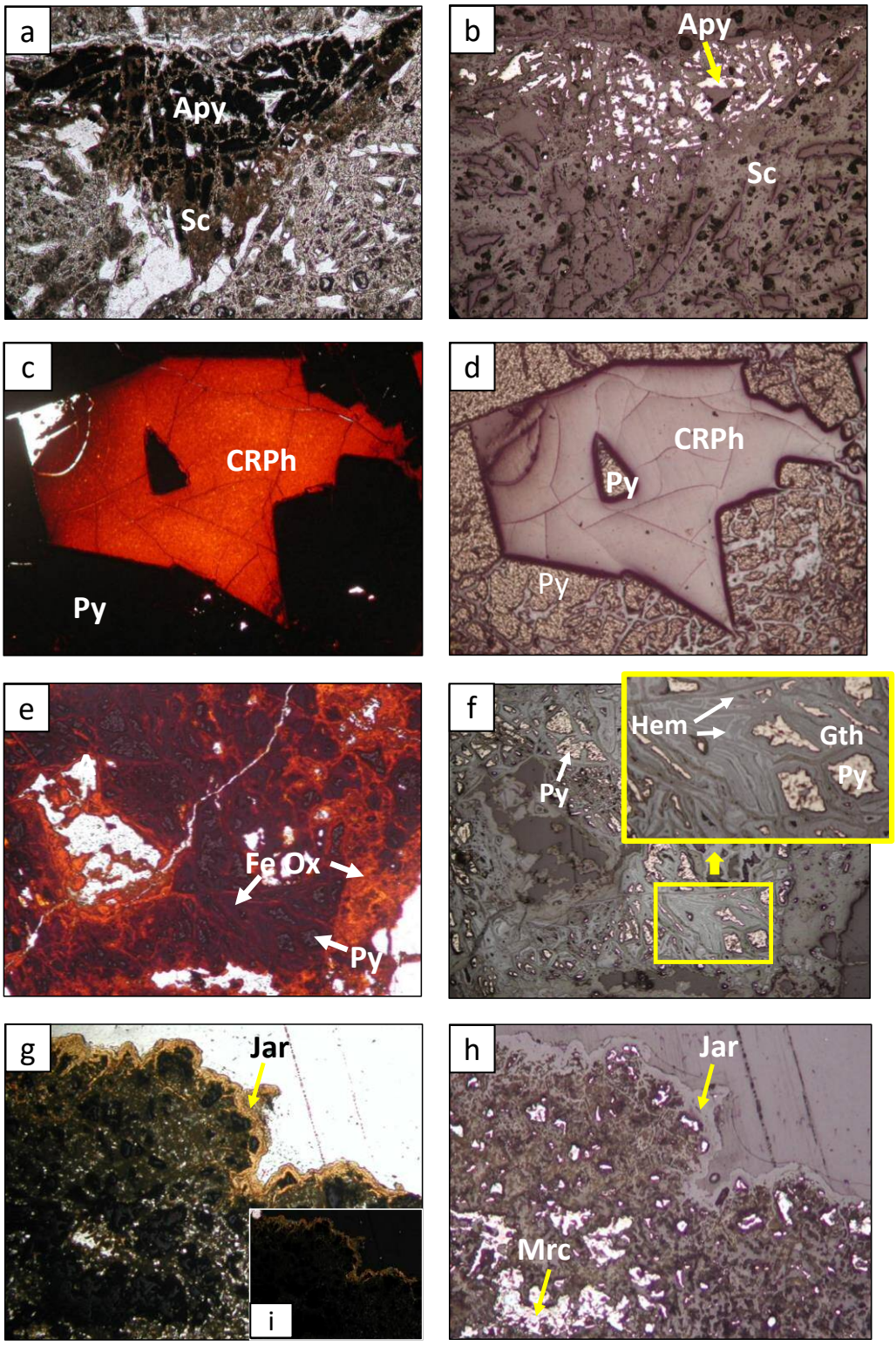
a
Apy
Sc
b
Apy
Sc
c
CRPh
Py
d
CRPh
Py
Py
e
Fe Ox
Py
f
Hem
Gth
Py
Py
g
Jar
i
h
Jar
Mrc

Figure 3.

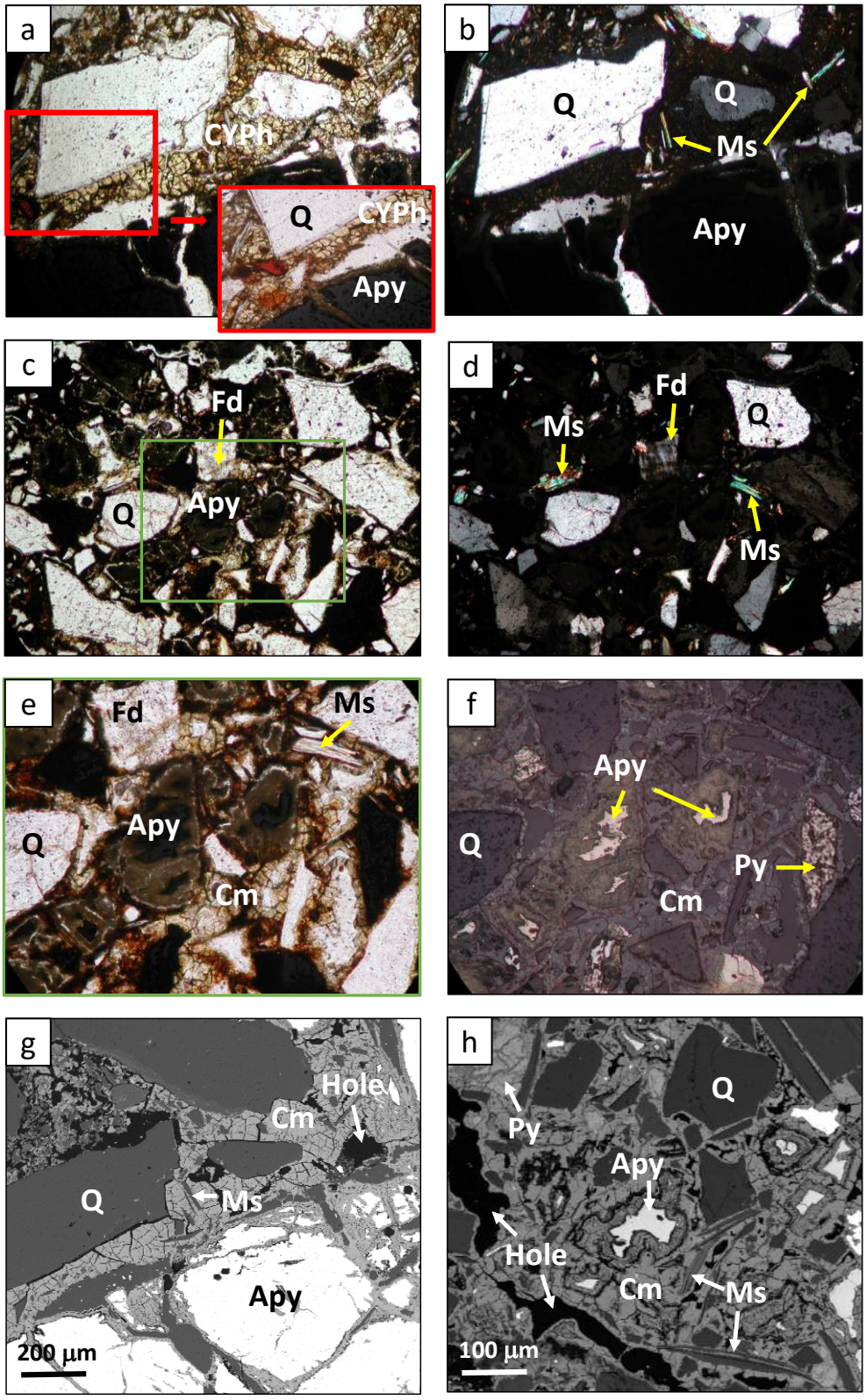
a
CYPh
Q
CYPh
Apy
b
Q
Q
Ms
Apy
c
Fd
Q
Apy
d
Fd
Ms
Q
Ms
e
Fd
Ms
Q
Apy
Cm
f
Apy
Q
Py
Cm
g
Hole
Cm
Q
Ms
Apy
200 µm
h
Q
Py
Apy
Hole
Cm
Ms
100 µm

Figure 4.

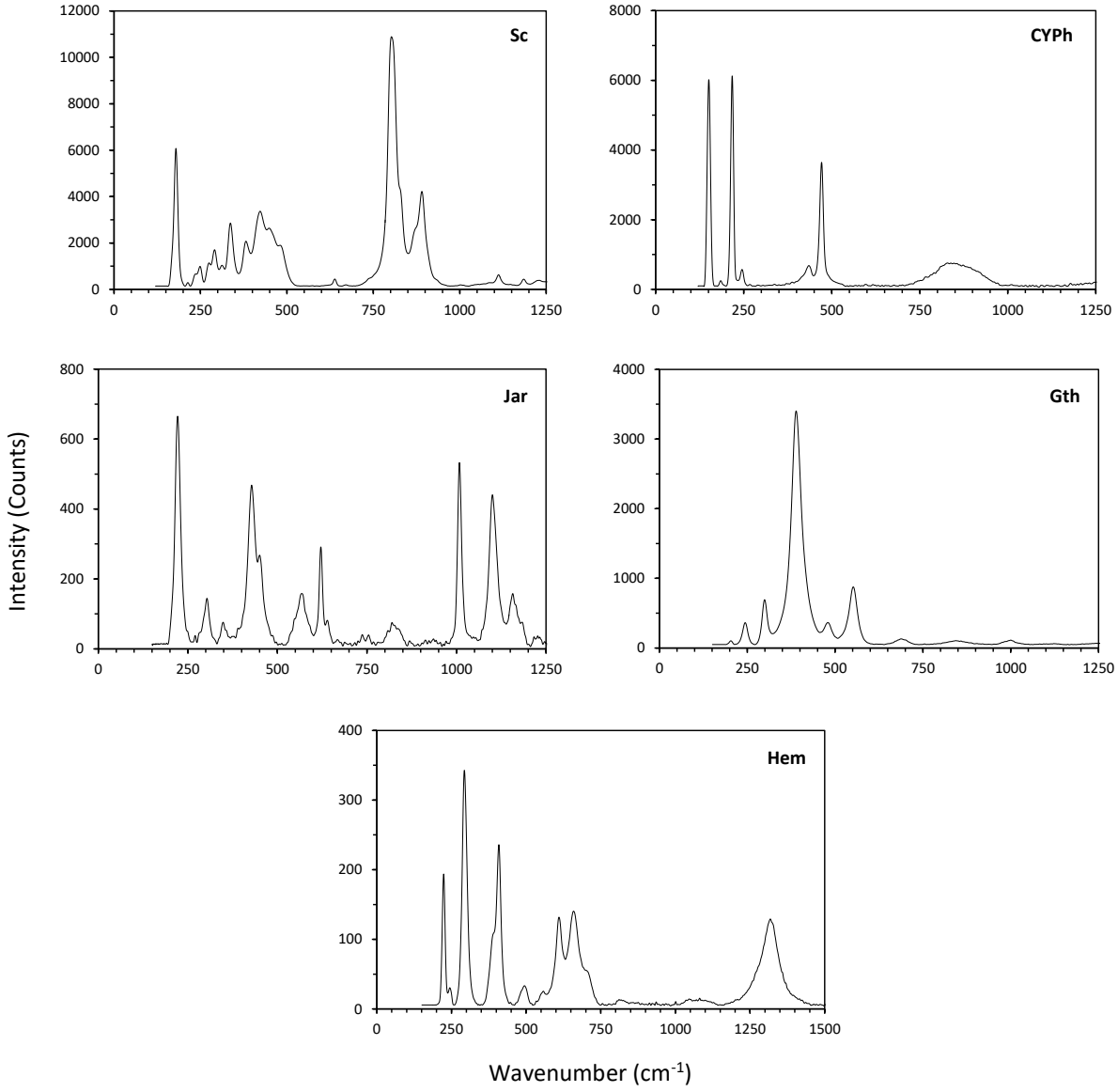

Figure 5.